Activated protein C modulates T-cell metabolism and epigenetic FOXP3 induction via α-ketoglutarate

Dheerendra Gupta,[1] Ahmed Elwakiel,[1] Satish Ranjan,[1] Manish Kumar Pandey,[1] Shruthi Krishnan,[1] Saira Ambreen,[1] Reinhard Henschler,[2] Rajiv Rana,[1] Maria Keller,[3,4] Uta Ceglarek,[1] Khurrum Shahzad,[1] Shrey Kohli,[1] and Berend Isermann[1]

[1]Institute of Laboratory Medicine, Clinical Chemistry, and Molecular Diagnostics and [2]Institute of Transfusion Medicine, University Hospital Leipzig, Leipzig University, Leipzig, Germany; [3]Helmholtz Institute for Metabolic, Obesity and Vascular Research (HI-MAG), Helmholtz Center Munich, University Hospital Leipzig, University of Leipzig, Leipzig, Germany; and [4]Medical Department III – Endocrinology, Nephrology, Rheumatology, University of Leipzig Medical Center, Leipzig, Germany

Key Points

- Coagulation protease aPC reduces *FOXP3* promoter methylation, inducing FOXP3 expression, and leading to Treg-like phenotype.

- The aPC-mediated induction of FOXP3 is linked to altered mitochondrial metabolism and reduced α-ketoglutarate and glutamine availability.

A direct regulation of adaptive immunity by the coagulation protease activated protein C (aPC) has recently been established. Preincubation of T cells with aPC for 1 hour before transplantation increases FOXP3$^+$ regulatory T cells (Tregs) and reduces acute graft-versus-host disease (aGVHD) in mice, but the underlying mechanism remains unknown. Because cellular metabolism modulates epigenetic gene regulation and plasticity in T cells, we hypothesized that aPC promotes FOXP3$^+$ expression by altering T-cell metabolism. To this end, T-cell differentiation was assessed in vitro using mixed lymphocyte reaction or plate-bound α-CD3/CD28 stimulation, and ex vivo using T cells isolated from mice with aGVHD without and with aPC preincubation, or analyses of mice with high plasma aPC levels. In stimulated CD4$^+$CD25$^-$ cells, aPC induces FOXP3 expression while reducing expression of T helper type 1 cell markers. Increased FOXP3 expression is associated with altered epigenetic markers (reduced 5-methylcytosine and H3K27me3) and reduced *Foxp3* promoter methylation and activity. These changes are linked to metabolic quiescence, decreased glucose and glutamine uptake, decreased mitochondrial metabolism (reduced tricarboxylic acid metabolites and mitochondrial membrane potential), and decreased intracellular glutamine and α-ketoglutarate levels. In mice with high aPC plasma levels, T-cell subpopulations in the thymus are not altered, reflecting normal T-cell development, whereas FOXP3 expression in splenic T cells is reduced. Glutamine and α-ketoglutarate substitution reverse aPC-mediated FOXP3$^+$ induction and abolish aPC-mediated suppression of allogeneic T-cell stimulation. These findings show that aPC modulates cellular metabolism in T cells, reducing glutamine and α-ketoglutarate levels, which results in altered epigenetic markers, Foxp3 promoter demethylation and induction of FOXP3 expression, thus favoring a Treg-like phenotype.

Introduction

The coagulation system is closely linked with inflammation in a reciprocal fashion. Yet, insight into the regulation of adaptive immunity by coagulation proteases has been provided only recently. In the context of

The full-text version of this article contains a data supplement.

graft-versus-host diseases (GVHD), a frequent complication after allogenic stem cell transplantation, the coagulation protease activated protein C (aPC) modulates the T-cell response in the acute GVHD (aGVHD) and chronic GVHD setting.[1,2] In aGVHD, aPC increases the frequency of FOXP3+ regulatory T cells (Tregs) through PAR2/PAR3-dependent signaling in T cells.[1] Intriguingly, a 1-hour preincubation with aPC before transplantation or allogenic stimulation of T cells was sufficient to increase FOXP3+ Treg frequency and reduce allogenic T-cell activation, dampening T-cell activation in vitro and the severity of, and inflammation in, aGVHD in vivo.

The protease aPC is efficiently generated by the complex of thrombomodulin and thrombin, but this process is impaired in the setting of endothelial dysfunction as observed in inflammation and GVHD.[3,4] Thus, loss of aPC generation because of endothelial dysfunction may provide an important microenvironmental cue, altering T-cell development and function.

The microenvironment, in part through cytokines and metabolites, is a strong modulator of T-cell development and function.[5-8] The development of FOXP3+ Tregs preferentially uses oxidative lipid metabolism, whereas effectors cells like T helper type 1 (Th1) cells require high glycolytic activity.[6,9-12] Thus, Treg development and function is less dependent on glucose and glycolysis than effector T-cell (Teff) development. Indeed, limited glucose availability increases Treg function, whereas high glucose uptake characterizes poorly suppressive Tregs.[13,14] T cells are metabolically flexible and can adapt to alternative substrates.[6] Thus, not only glucose but also glutamine act as metabolic substrates, increasing tricarboxylic acid (TCA) cycle metabolites such as α-ketoglutarate (α-KG).[6] Increased levels of α-KG promote the proliferation of Teffs, whereas limiting α-KG promotes Treg development.[15,16] α-KG and other metabolites have multiple functions, including modification of epigenetic regulators and, thus, linking intracellular metabolism to T-cell development and function.[17]

Although the effect of microenvironmental metabolic cues on T-cell development is established, it remains unknown to which extent coagulation proteases modulate these processes. Epigenetic gene regulation by coagulation proteases has been demonstrated for aPC in the setting of chronic vascular complications such as diabetic kidney disease and atherosclerosis.[18-20] However, the mechanism through which aPC modulates epigenetic gene expression and whether this relates to altered cellular metabolism remains unknown.

Given (i) that 1-hour preincubation of T cells with aPC is sufficient to induce Tregs and to dampen GVHD,[1] (ii) that aPC epigenetically regulates expression of some genes in the setting of chronic vascular diseases,[18-20] (iii) the established role of T-cell metabolism in regulating T-cell differentiation,[6,9,10,12] and (iv) the role of cellular metabolism in the epigenetic control of T-cell development[21,22] we hypothesized that FOXP3 induction upon incubation of T cells with aPC depends on altered cellular metabolism and associated epigenetically controlled T-cell differentiation.

Methods

Mice

Wild-type (WT) C57BL/6 mice were purchased from Janvier S.A.S., St Berthevin Cedex, France. Transgenic APC^high mice (8 to 10-weeks old) expressing a human PC variant (D167F/D172K), which can be efficiently activated in the absence of thrombomodulin, resulting in elevated aPC plasma concentrations, have been described previously.[1,23] Depletion of regulatory T cell (DEREG) mice have been described previously[24] and were backcrossed onto the C57BL/6 background for at least 10 generations. All animal experiments were conducted in accordance with standards and procedures approved by the local animal care and use committee (Landesverwaltungsamt Halle and Landesverwaltungsamt Leipzig, Germany).

Human

All blood samples were collected from healthy donors in accordance with the Declaration of Helsinki and Good Clinical Practice Guidelines and with approval by the ethics committee (Ethics commission of Medical Faculty, Leipzig University, Germany) and the relevant regulatory authority (University Hospital Leipzig, Germany). All participants provided written informed consent.

Cell isolation and mixed lymphocyte culture

To conduct the mixed lymphocyte reaction (MLR), human CD4+CD25− cells were cultured with non-T cells containing antigen-presenting cells. To isolate human CD4+CD25− cells, peripheral blood mononuclear cells were isolated from peripheral blood using a Ficoll-Paque (GE Healthcare) gradient, after which non-T cells were depleted by magnetic beads using a MojoSort human pan T-cell isolation kit following the manufacturer's protocol. Pan T cells were subjected to a human CD4+CD25+CD127^dim/− Regulatory T-Cell Isolation Kit II (Miltenyi Biotec), providing human CD4+CD25+ Tregs and untouched CD4+CD25− cells. This CD4+CD25− population is devoid of Tregs. Fluorescence-activated cell sorting was used to determine cell purity, which ranged from 95% to 98%. Non-T cells were irradiated (30 Gy) and used as antigen-presenting cells.

Human CD4+CD25− cells were cultured in AIM V serum-free medium (Life Technologies) for 2 hours (37°C, 5% CO_2) before performing the MLR. To trigger allogenic T-cell reactions in the MLR, CD4+CD25− cells and non-T cells from 2 genetically distinct individuals were cocultured. In some experiments, 1×10^5 CD4+CD25− cells were preincubated with aPC (20 nM) or an equal volume of phosphate-buffered saline (PBS) (control) in AIM V serum-free medium (1 hour, 37°C), washed with PBS to remove any aPC, and then cocultured with 3×10^5 irradiated allogenic non-T cells (ratio, 1:3) for 96 hours.

Plate-bound stimulation was carried out by coating plates with αCD3 and αCD28 for 2 hours at 37°C followed by washing of the plate with PBS. T cells were seeded onto plates without or with aPC preincubation (1 hour, 20 nM). In some experiments, cells were supplemented with cell-permeable α-KG (dimethyl α-KG; 3.5 mM; Sigma-Aldrich) and glutamine (4 mM; Sigma-Aldrich) during stimulation.

Statistics

Results are expressed as mean ± standard error of the mean from (n) independent experiments. Each in vitro experiment was conducted in triplicates and dots in bar graphs reflect the average from such triplicates. For in vivo experiments, each dot represents data from 1 mouse. Statistical analyses were performed with the Student t test or analysis of variance, as appropriate and indicated in

the figure legends. Post hoc comparisons of analysis of variance were corrected with the method of Bonferroni, as indicated in figure legends. Prism 8 software (GraphPad Software, San Diego, CA) was used for statistical analysis. Values of $P < .05$ were considered statistically significant.

Additional information is available in the supplemental Material.

Results

aPC induces FOXP3 Tregs via epigenetic modulation

Preincubation of magnetically sorted CD4$^+$CD25$^-$ T cells with aPC followed by stimulation with plate-bound αCD3 and αCD28 increased CD4$^+$FOXP3$^+$ cell abundance after 96 hours (Figure 1A; supplemental Figure 1A), which is congruent with observations in allogeneically stimulated pan T cells.[1] Other surface Treg markers like CTLA4, PD-1, and LAG3 were also increased upon aPC preincubation, corroborating the induction of a Treg-like phenotype upon aPC preincubation (supplemental Figure 1B-D). The increased frequency of CD4$^+$FOXP3$^+$ cells was associated with a reduction in CD4$^+$T-bet$^+$ andCD4$^+$IFNγ$^+$ cell abundance (Figure 1B-C). As magnetic separation of the CD4$^+$CD25$^-$ cell population can contain different memory T-cell populations, which might contribute to Treg induction,[25] we determined the effect of aPC on purified naïve T cells under Treg polarization conditions (supplemental Figure 2A). Preincubation of naïve T cells with aPC likewise induced FOXP3 expression, which corresponds with increased CD4$^+$CD25$^+$FOXP3$^+$ frequency, reflecting the observations made in CD4$^+$CD25$^-$ cells (Figure 1D; supplemental Figure 2B-D). Collectively, the induction of FOXP3 expression in pan T cells,[1] in CD4$^+$CD25$^-$ cells (Figure 1A), and in naïve T cells (Figure 1D) support a model in which pretreatment of T cells with aPC induces expression of FOXP3 and promotes Treg-like cells.

Given that a 1-hour preincubation with aPC is sufficient for induction of FOXP3 and Treg marker expression and that the Treg transition from Th1/Th17/T-conventional cells is linked to epigenetic reprogramming,[15,26,27] we assessed whether aPC modifies the epigenetic markers in αCD3/αCD28-stimulated CD4$^+$CD25$^-$ cells. Indeed, global 5-methylcytosine levels were decreased in aPC-preincubated CD4$^+$CD25$^-$ cells compared with those in control CD4$^+$CD25$^-$ cells 48 hours after αCD3/αCD28 stimulation (Figure 1E). In parallel, global H3K27me3 levels, a repressive marker associated with transcriptionally silenced genes, were decreased in aPC-preincubated CD4$^+$CD25$^-$ cells (Figure 1F). Furthermore, compared with control CD4$^+$CD25$^-$ cells, methylation of different regions of the *FOXP3* promoter was markedly reduced by preincubation with aPC of CD4$^+$CD25$^-$ cells stimulated with αCD3 and αCD28 (Figure 1G-H). These results suggest that the aPC-mediated changes in the epigenetic landscape of T cells lead to induction of FOXP3 expression.

Preincubation with aPC alters mitochondrial metabolism in CD4$^+$CD25$^-$ T cells

Epigenetic modifications in T cells are closely linked to cellular and mitochondrial metabolism.[21,22] Therefore, we observed mitochondrial metabolism in stimulated T cells with or without 1-hour aPC preincubation. We used 2 independent experimental approaches: CD4$^+$CD25$^-$ cells stimulated (i) with plate-bound αCD3/αCD28,

or (ii) in a MLR (Figure 2A-B). The oxygen consumption rate (OCR), reflecting mitochondrial metabolism, was analyzed using the Seahorse analyzer. Parameters of mitochondrial respiration (OCR, comprising basal and maximal respiration, spare respiratory capacity, and adenosine triphosphate production) were reduced in aPC-preincubated T cells compared with control T cells in both experimental settings (Figure 2A-B; supplemental Figure 3A-C). The reduced OCR in aPC-preincubated CD4$^+$CD25$^-$ cells was paralleled by a reduced extracellular acidification rate (ECAR), representing glycolysis, suggesting that aPC induces metabolic quiescence in T cells (Figure 2C; supplemental Figure 3D).

Next, we determined whether reduced mitochondrial oxygen consumption is associated with a reduction in mitochondrial activity in aPC-preincubated T cells. Pretreatment of CD4$^+$CD25$^-$ cells with aPC reduced the mitochondrial membrane potential (ΔΨm) relative to that of control cells (Figure 2D). Taken together, these data suggest that aPC induces metabolic quiescence in association with reduced mitochondrial metabolism and mitochondrial membrane potential in T cells, which may promote FOXP3 Treg induction.

aPC reduces intracellular α-KG levels in T cells

Because metabolites of the TCA cycle modulate T-cell fate,[15,16,21] we studied TCA metabolites. Pretreatment of CD4$^+$CD25$^-$ cells with aPC followed by αCD3/αCD28 stimulation for 24 hours reduced pyruvate, citrate, and α-KG levels in T cells (Figure 3A). The reduction of pyruvate, the end metabolite of glycolysis, is congruent with the reduced ECAR and metabolic quiescence in aPC-preincubated CD4$^+$CD25$^-$ cells. Congruent with the reduced ECAR and pyruvate levels in preincubated CD4$^+$CD25$^-$ cells, aPC reduced *GLUT1* expression and glucose uptake in CD4$^+$CD25$^-$ cells (Figure 3B-C).

α-KG, a TCA metabolite known to regulate enzymatic epigenetic modifiers, can also be derived from glutaminolysis in an anaplerotic reaction (Figure 3D).[16,28-30] The reduction of α-KG levels suggest that its deficiency is not compensated by glutaminolysis. Hence, we ascertained whether aPC affects intracellular glutamine and glutamate levels. In comparison with control CD4$^+$CD25$^-$ cells, both glutamine and glutamate were reduced in aPC-preincubated CD4$^+$CD25$^-$ cells (Figure 3E). This reduction was associated with reduced expression of *SLC1A5* and *SLC38A1*, 2 key amino acid transporters (Figure 3F).[31-34] Thus, aPC reduces intracellular α-KG availability by simultaneously suppressing glucose uptake and the anaplerotic glutamine-dependent reaction.

α-KG or glutamine reverses the effect of aPC on mitochondrial metabolism in CD4$^+$CD25$^-$ cells

Because the reduced availability of glutamine and α-KG increases FOXP3 expression, leading to induction of FOXP3 Treg frequency,[16,22] we examined the functional relevance of reduced α-KG and glutamine for aPC's effect on T cells by substituting cell-permeable α-KG (dimethyl α-KG) or glutamine. After 24 hours of stimulation with αCD3 and αCD28, the OCR was measured in both control and aPC-preincubated CD4$^+$CD25$^-$ cells (Figure 4A). The reduction of mitochondrial metabolism as reflected by the OCR and OCR-derived parameters were abolished upon exogenous supplementation of cell-permeable α-KG or glutamine in aPC-preincubated CD4$^+$CD25$^-$ cells (Figure 4). Thus, substituting
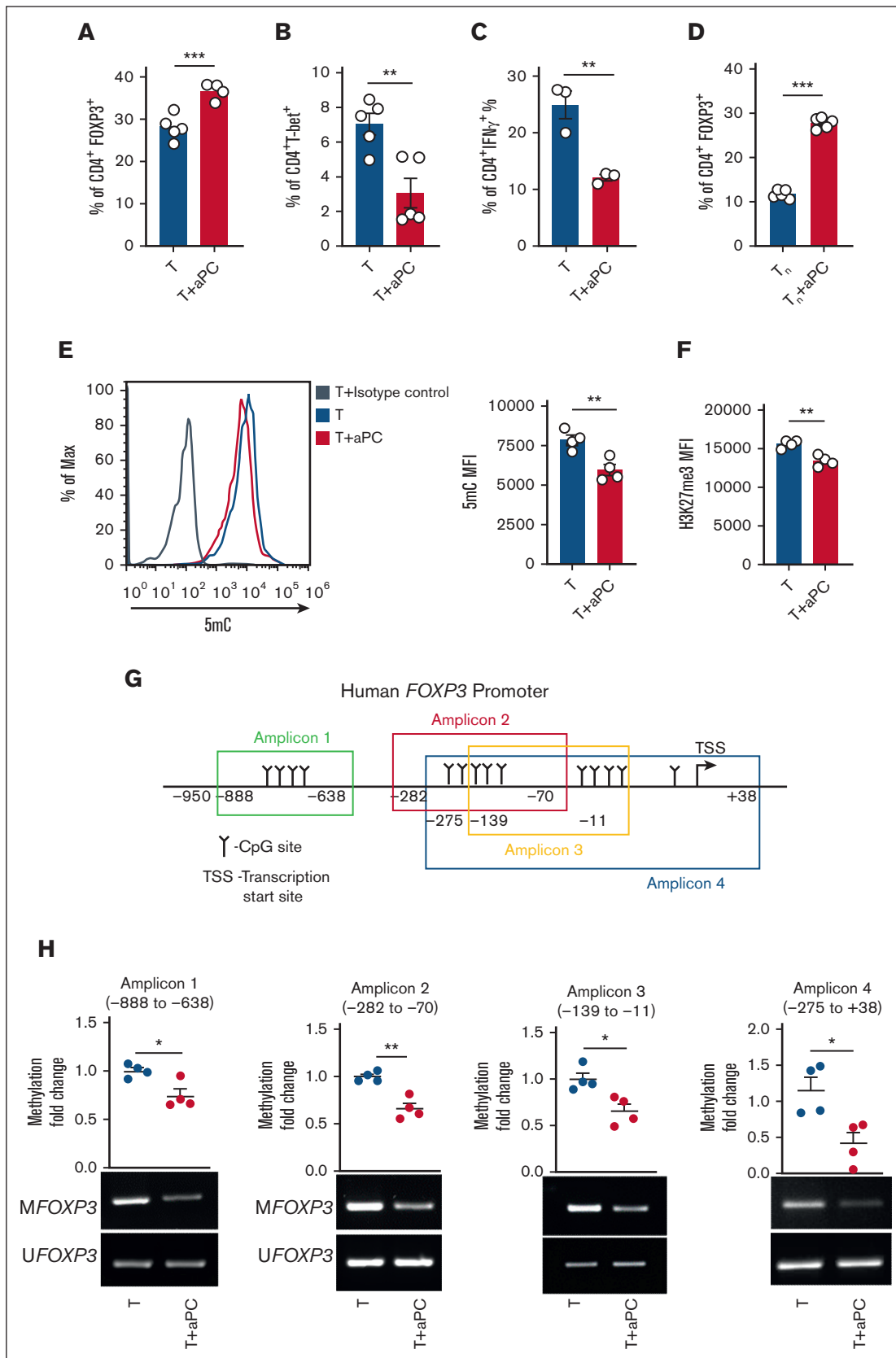
Figure 1. aPC reduces *FOXP3* promoter methylation. (A-C) Frequencies of CD4$^+$FOXP3$^+$ (A), CD4$^+$T-bet$^+$ (B), and CD4$^+$IFNγ$^+$ (C) cells without (T) or with aPC (T + aPC) preincubation (1 hour, 20 nM) as determined by flow cytometry 96 hours after activation of human CD4$^+$CD25$^-$ cells with αCD3 and αCD28 (A-B, n = 5; C, n = 3). Bar graphs

blood advances

α-KG or glutamine restores mitochondrial metabolism in aPC-preincubated αCD3/αCD28-stimulated CD4$^+$CD25$^-$ cells.

The aPC-induced Treg-like phenotype is reversed upon substitution of α-KG or glutamine

Using human CD4$^+$CD25$^-$ cells, we investigated the effect of α-KG and glutamine in an MLR without and with aPC for 96 hours. FOXP3 induction by aPC was prevented upon addition of either α-KG or glutamine (Figure 5A; supplemental Figure 4A). In parallel, the aPC-induced suppression of T-bet and interferon γ, markers reflecting Th1/Teff cells, was reversed upon the supplementation of α-KG and glutamine (Figure 5B-C; supplemental Figure 4B-C). Thus, supplementation of exogenous α-KG or glutamine reverses the aPC-dependent induction of a Treg-like phenotype.

aPC suppresses T-cell proliferation by inducing Tregs.[1] To determine whether the supplementation of α-KG and glutamine abolishes this effect of aPC, we studied the proliferation of CD4$^+$CD25$^-$ cells in a MLR without or with aPC preincubation. Indeed, the suppression of proliferation in aPC-preincubated T cells was prevented by α-KG and glutamine supplementation. (Figure 5D-E). Taken together, these results support a model in which aPC promotes FOXP3$^+$ Tregs by reducing α-KG and glutamine availability.

aPC modifies the epigenetic and metabolic profile in murine CD4$^+$CD25$^-$ cells, promoting a Treg-like phenotype

Because genetic manipulation of primary human T cells and in vivo interventions in humans are challenging, we evaluated whether aPC induces a Treg-like phenotype in mouse T cells via metabolic reprogramming. In mouse CD4$^+$CD25$^-$ cells, preincubation with aPC (1 hour, 20 nM) reduced global 5-methylcytosine levels after 48 hours of αCD3 and αCD28 stimulation (Figure 6A), reflecting the observations in human CD4$^+$CD25$^-$. Moreover, preincubation with aPC decreased Foxp3 promoter methylation in mouse CD4$^+$CD25$^-$ compared with control cells (Figure 6B), mirroring the observations in human T cells. Pyrosequencing analyses of 5 CpG sites within the murine Foxp3 promoter revealed reduced methylation of all tested 5 CpG sites in aPC-preincubated αCD3/αCD28-stimulated CD4$^+$CD25$^-$ cells (Figure 6C). To determine the functional relevance of reduced promoter methylation, we transfected a murine T-cell line (EL4 cells) with a Foxp3 promoter-driven luciferase reporter construct. Preincubation with aPC before αCD3/αCD28 stimulation increased the promoter activity compared with that in control cells (Figure 6C). Thus, preincubation of CD4$^+$CD25$^-$ cells with aPC reduces Foxp3-promoter methylation, which translates into increased Foxp3-promoter activity.

Next, to determine whether the aPC-induced metabolic changes observed in stimulated human T cells (plate-bound αCD3/αCD28 or MLR) can be recapitulated in a disease setting, we isolated T cells from mice with GVHD. Following our previously established protocol,[1] T cells were preincubated with aPC for 1 hour before transplantation and OCR parameters were analyzed ex vivo after 2 weeks. In comparison with control T cells, aPC-preincubated T cells had lower levels of basal and maximal respiration and adenosine triphosphate generation, whereas there was no significant change in spare respiratory capacity (Figure 6E; supplemental Figure 5). Thus, aPC-preincubation of murine T cells before transplantation reduces mitochondrial respiration after induction of GVHD, reflecting the observations made in activated human T cells preincubated with aPC.

To determine whether the aPC-mediated induction of the Treg-like phenotype depends on the altered cellular metabolism, we exogenously supplemented α-KG or glutamine in mouse T-cell culture. To this end, we used DEREG mice, which express green fluorescent protein (GFP) under the control of a Foxp3 promoter, allowing detection of Foxp3 promoter activity in primary cells. CD4$^+$GFP$^-$ cells isolated from these mice were subjected to ex vivo stimulation with plate-bound αCD3/αCD28, and the frequency of GFP$^+$ cells was determined after 96 hours. aPC increased the frequency of CD4$^+$GFP$^+$ cells, reflecting increased FoxP3 promoter activity upon aPC pretreatment (Figure 6F). The aPC-mediated induction of CD4$^+$GFP$^+$ T cells was markedly reduced in the presence of α-KG or glutamine (Figure 6F), demonstrating that the induction of FoxP3 promoter activity depends on the reduced availability of α-KG and glutamine.

aPC dampens T-cell metabolism and increases peripheral CD4$^+$FOXP3$^+$ cell frequency in vivo

To determine whether aPC affects T-cell development in vivo, we analyzed APC^{high} mice that express a hyperactivatable PC variant resulting in increased aPC levels.[23] APC^{high} mice are protected from GVHD, which is associated by FOXP3 induction and increased Treg frequency.[1] Analysis of thymocytes revealed no differences between WT and APC^{high} mice (supplemental Figure 6A-B). Thus, the frequency of CD4$^+$ and CD8$^+$ single-positive and double-positive T cells were comparable in the thymus of WT and APC^{high} mice (supplemental Figure 6C). Further analyses demonstrated that also naïve T cells (CD62L$^+$ CD44$^-$), central memory T cells (CD62L$^+$ CD44$^+$), and Teffs (CD62L$^-$CD44$^+$) in the thymus were comparable among WT and APC^{high} mice (supplemental Figure 6D-E). Congruent with normal T-cell development, the frequency of CD4$^+$FOXP3$^+$ (Tregs) cells in the thymus was comparable in APC^{high} mice and WT mice, whereas the CD4$^+$FOXP3$^+$ frequency in the spleen was increased

Figure 1 (continued) with dot plots summarizing data. (D) Frequency of CD4$^+$FOXP3$^+$ cells without (T$_n$) or with aPC (T$_n$ + aPC) preincubation (1 hour, 20 nM) under Treg polarization condition as assessed by flow cytometry 5 days after activation of human naïve T cells (T$_n$) with αCD3 and αCD28 (n = 5). Bar graphs with dot plots summarizing data. (E-F) Global methylation changes, as reflected by 5-methylcytosine (5mC) (E, n = 4, human), and H3K27Me3 (F, n = 4, human) in CD4$^+$CD25$^-$ cells without (T) or with aPC (T + aPC) preincubation followed by stimulation with αCD3 and αCD28 for 48 hours. Representative histogram (E, left) and bar graph with dot plot (E, right; F) summarizing the results from flow cytometry as the mean fluorescence intensity (MFI). (G-H) Schematic representation of human FOXP3 promoter showing CpG sites in different regions and amplicons used for methylation-specific polymerase chain reaction (PCR) (MSP) (G). FOXP3 promoter methylation of different regions (methylation-specific PCR, n = 4 each group, H) and dot plot summarizing results of MSP in the FOXP3 promoter in human CD4$^+$CD25$^-$ cells without (T) or with aPC (T + aPC) preincubation (1 hour, 20 nM) followed by 48 hours of stimulation with αCD3 and αCD28. The data are shown as the mean ± standard error of the mean (SEM); statistical significance was determined by 2-tailed Student t test (A-H): *$P < .05$, **$P < .01$, and ***$P < .005$.
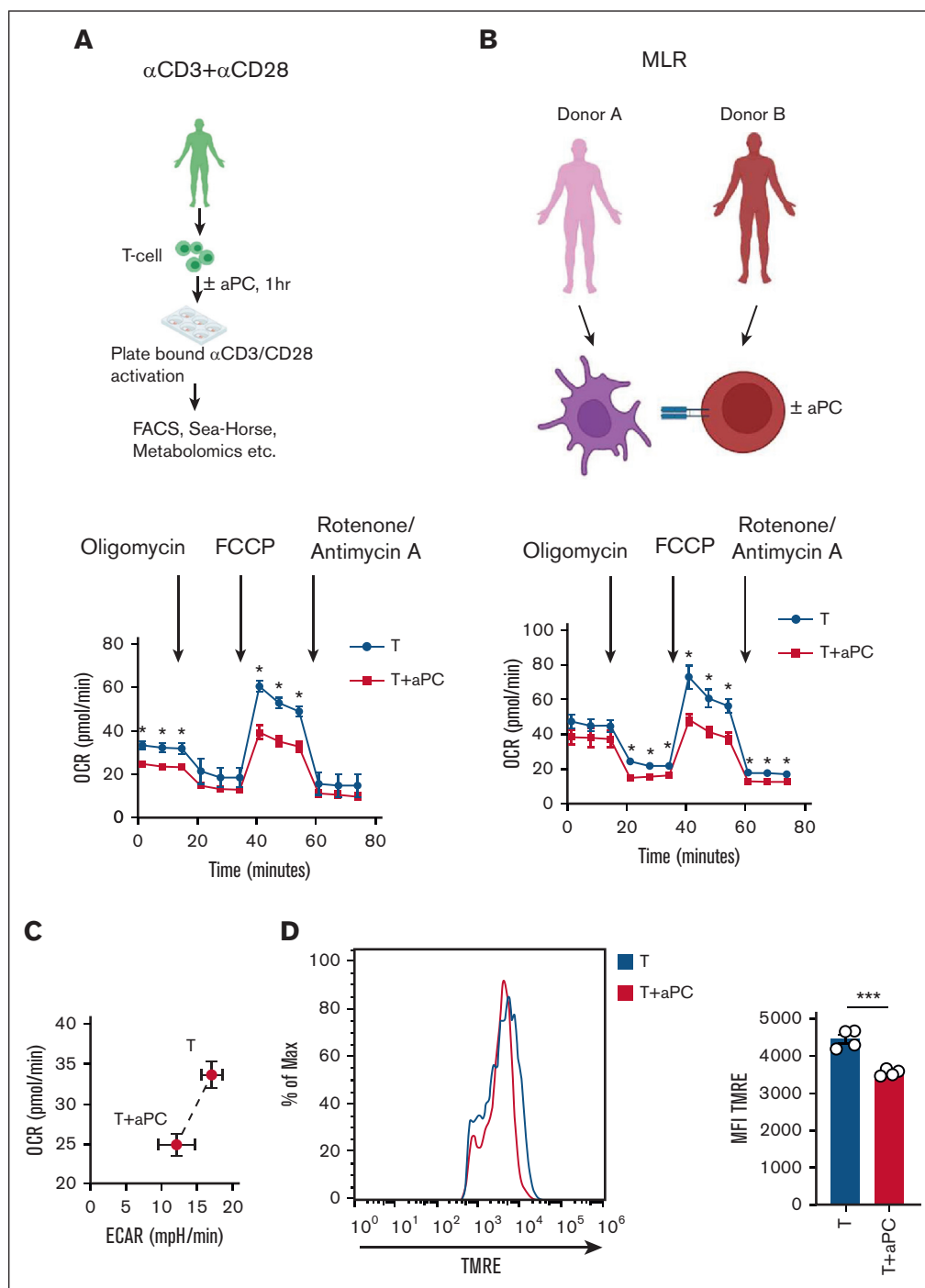
Figure 2. aPC preincubation reduces mitochondrial respiration in CD4$^+$CD25$^-$ cells. (A-B) Independent experimental approaches to study mitochondrial metabolism in stimulated T cells: stimulation of human CD4$^+$CD25$^-$ cells by plate-bound αCD3 and αCD28 for 48 hours (A, top); stimulation of human CD4$^+$CD25$^-$ cells using an MLR (48 hours) (B, top). In both cases, T cells were preincubated with aPC (20 nM, 1 hour) before stimulation (plate-bound αCD3 and αCD28, or MLR). Representative line graph showing OCR (A-B; bottom) (A, n = 3; B, n = 5). (C) Seahorse analysis showing bioenergetics profile of CD4$^+$CD25$^-$ cells (OCR vs ECAR; energy graph) 48 hours after stimulation with αCD3 and αCD28 without (T) or with aPC preincubation (T + aPC). (D) Representative flow cytometry histogram (MFI, left) and bar graph with dot plot quantifying the percentage of tetramethylrhodamine ethyl ester (TMRE)-positive cells (flow cytometry, right) reflecting the mitochondrial membrane potential in human CD4$^+$CD25$^-$ cells preincubated without or with aPC (n = 4). The data are shown as the mean ± SEM, and statistical significance was determined by a 2-tailed Student t test. ***$P < .005$. Images in panels A-B were created using BioRender.com.
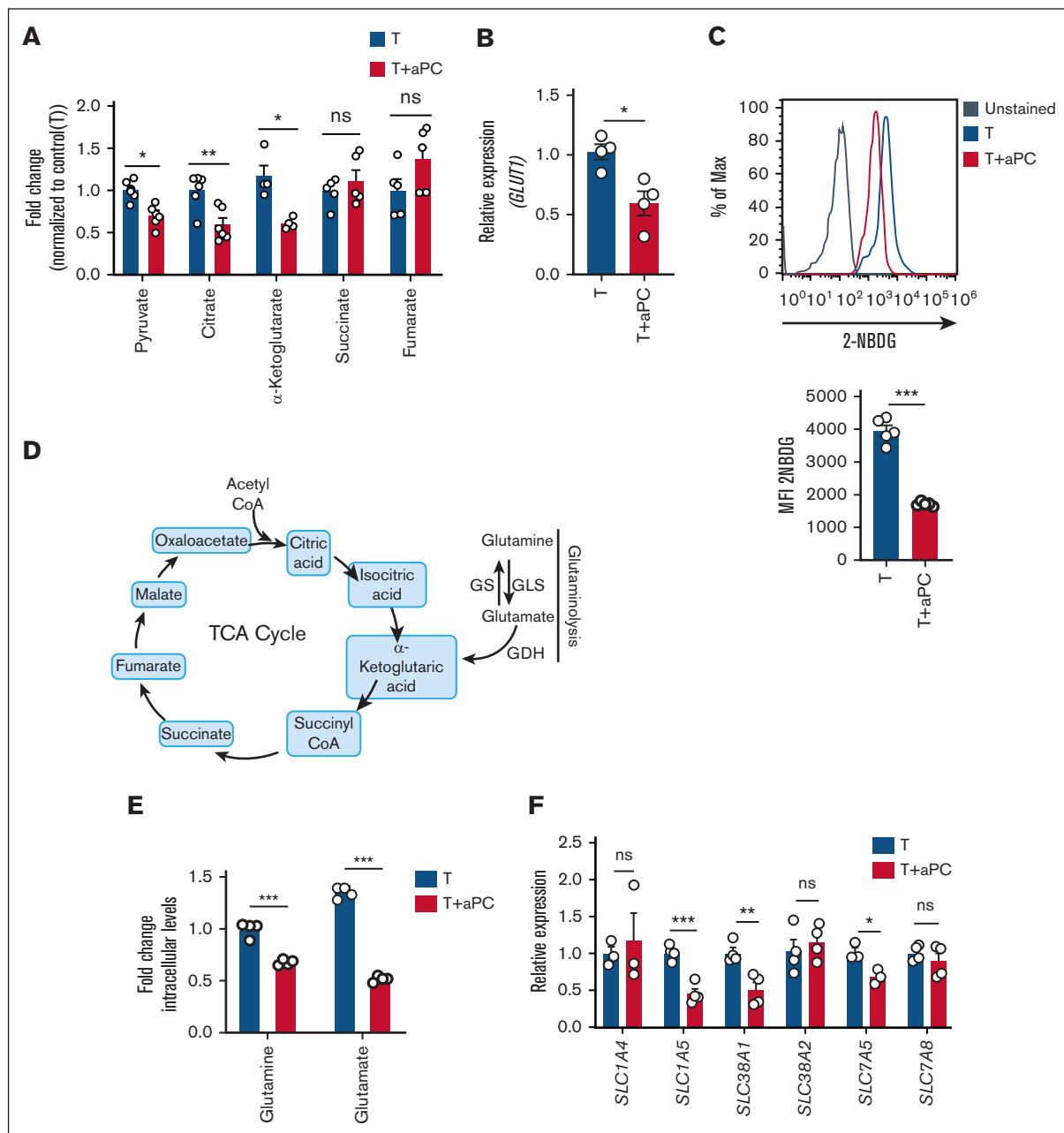
Figure 3. aPC reduces α-KG and glutamine in T cells. (A) Bar graph with dot plot of TCA cycle metabolites (liquid chromatography mass spectrometry [LC-MS] analysis, n = 5) in human CD4$^+$CD25$^-$ cells 24 hours after stimulation with αCD3 and αCD28 without (T) or with aPC (T + aPC) preincubation. (B-C) Bar graph with dot plot summarizing gene expression (messenger RNA [mRNA], quantitative PCR [qPCR]) of the glucose transporter *GLUT1* (B, n = 4) and representative flow cytometry histogram (top) and bar graph with dot plot summarizing glucose (fluorescently labeled glucose, 2-(*N*-(7-nitrobenz-2-oxa-1,3-diazol-4-yl)amino)-2-deoxyglucose [2-NBDG], below) uptake into human CD4$^+$CD25$^-$ cells 24 hours after stimulation with αCD3 and αCD28 without (T) or with aPC (T + aPC) preincubation (n = 4). (D) Cartoon depicting the fueling of α-KG via glutaminolysis. (E-F) Bar graph with dot plot summarizing intracellular levels of glutamine and glutamate (E, LC-MS analysis, n = 4) and gene expression (mRNA, qPCR) of amino acid transporters (F, n = 3) in human cells as described for panel A. The data are shown as the mean ± SEM, and statistical significance was determined by a 2-tailed Student *t* test for the panels A-C,E-F: *$P < .05$, **$P < .01$, and ***$P < .005$; ns, nonsignificant. Cartoon for panel D was created using BioRender.com.

in APC^{high} mice (Figure 7A). Collectively, these results show that primary T-cell development is not altered in APC^{high} mice, whereas aPC promotes FOXP3 Treg development in peripheral lymphoid organs.

Because aPC reduces α-KG and glutamine availability in T cells in vitro, we determined whether T-cell metabolism is altered in T cells of APC^{high} mice. Upon αCD3/αCD28 stimulation, mitochondrial metabolism (as reflected by OCR-related parameters) was
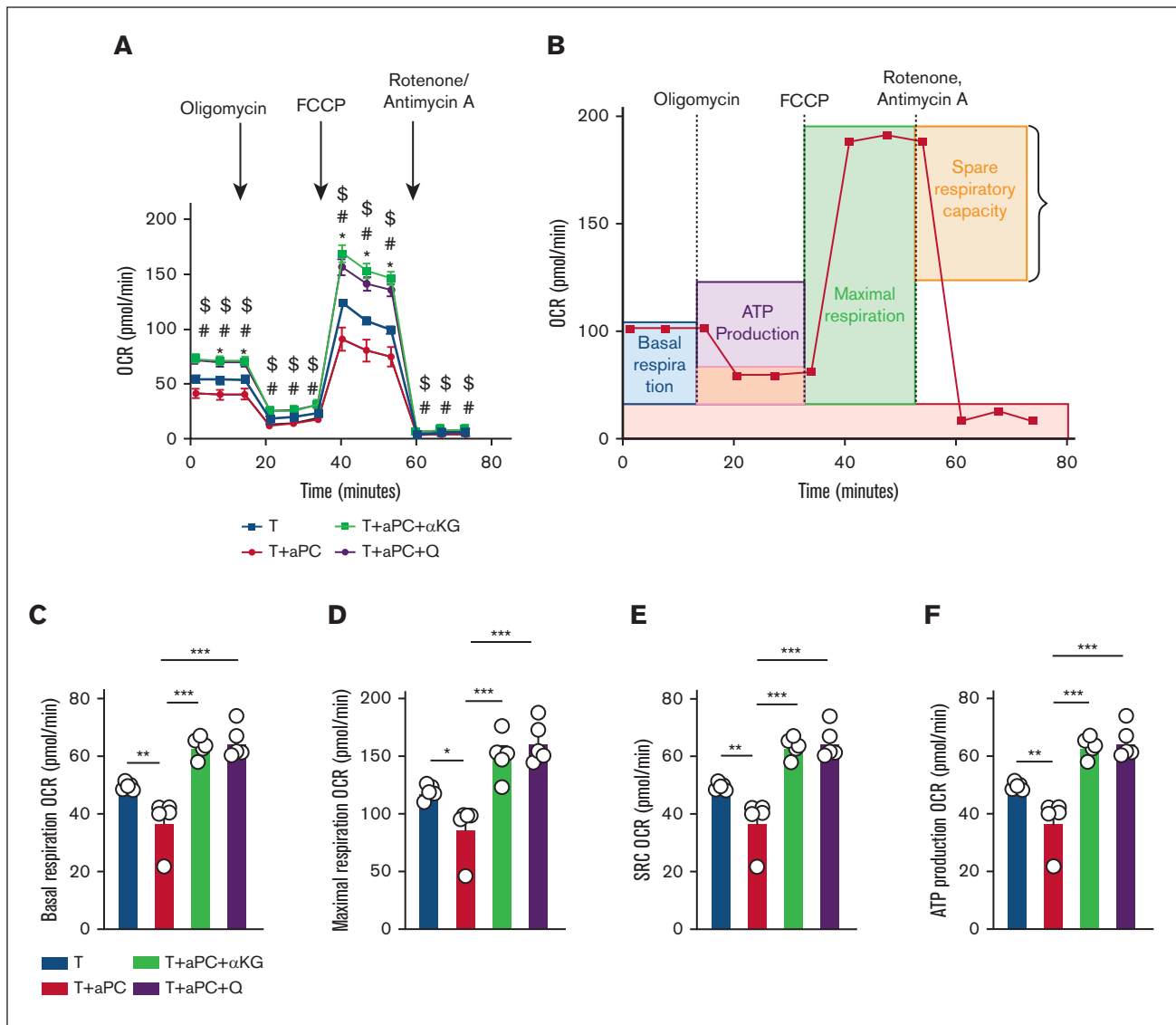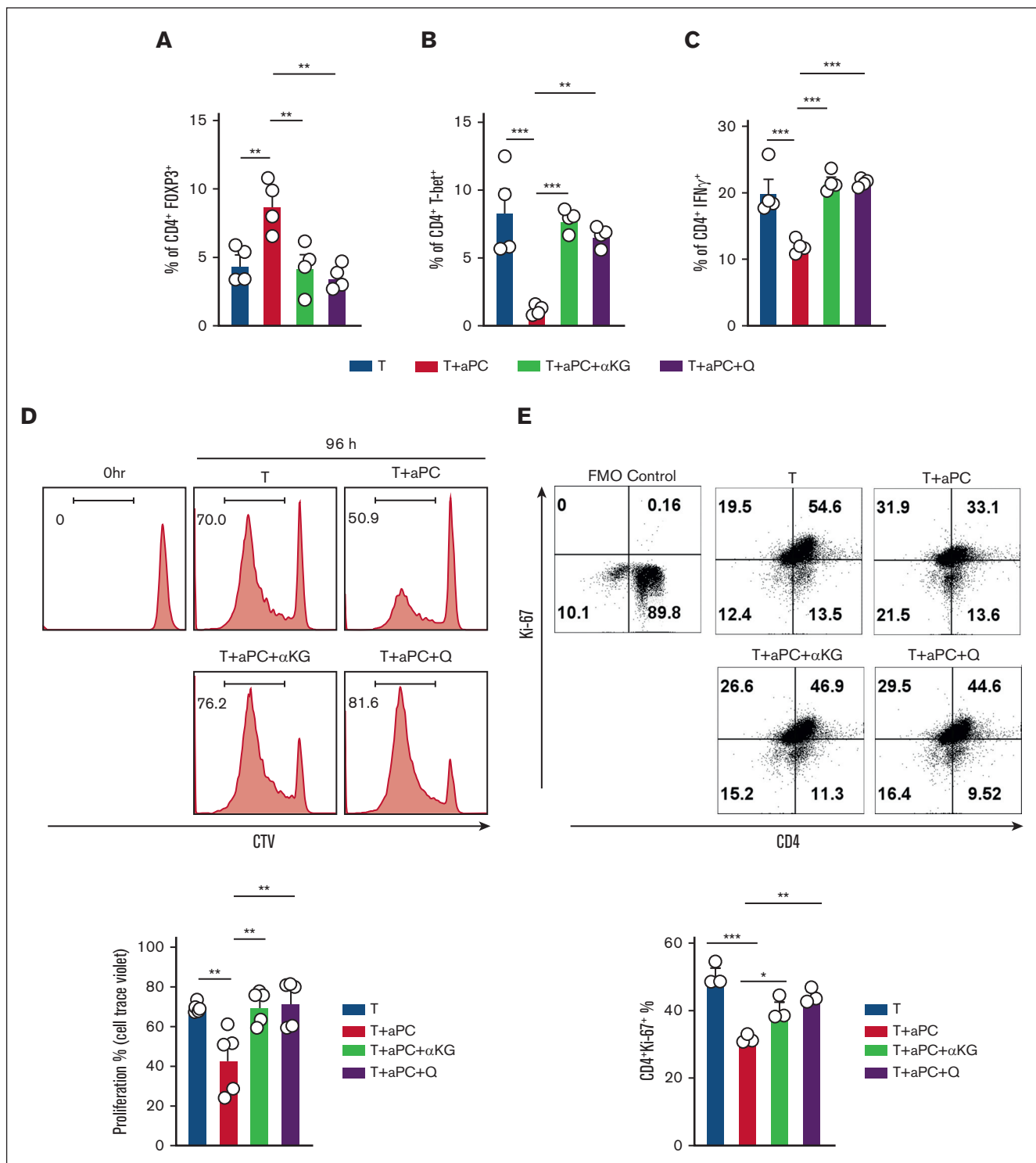
Figure 4. Reversal of aPC's effect on mitochondrial metabolism in CD4$^+$CD25$^-$ cells by α-KG or glutamine supplementation. (A) Line graph showing Seahorse analysis of OCR in human CD4$^+$CD25$^-$ cells preincubated without (T) and with aPC alone (T + aPC; 1 hour, 20 nM) or with supplementation of α-KG (48 hour, 3.5 mM, T + aPC + α-KG) or glutamine (48 hours, 4 mM, T + aPC + Q). (B) Schematic line plot showing the areas of the OCR curves representing basal respiration, maximum respiration, spare respiratory capacity (SRC), and adenosine triphosphate (ATP) production. (C-F) Bar graphs with dot plots summarizing basal respiration (C), maximal respiration (D), SRC (E), and ATP production (F) (n = 5) in experimental groups as described in panel A. The data are shown as the mean ± SEM; statistical significance was determined by 2-way analysis of variance (ANOVA) for panel A or 1-way ANOVA for panels C-F. Significance is represented in panel A: *$P < .05$ (T vs T + aPC), #$P < .05$ (T + aPC vs T + aPC + α-KG), $\$P < .05$ (T vs T + aPC + Q); and panels C-F: *$P < .05$, **$P < .01$, and ***$P < .005$.

reduced in CD4$^+$CD25$^-$ cells from APC^{high} mice compared with CD4$^+$CD25$^-$ cells from WT mice (Figure 7B; supplemental Figure 6F). To determine whether the reduced OCR in APC^{high}-derived CD4$^+$CD25$^-$ cells and increased CD4$^+$FOXP3$^+$ cell frequency in APC^{high} mice depend on reduced availability of α-KG, we supplemented α-KG in cultured CD4$^+$CD25$^-$ cells obtained from APC^{high} mice ex vivo. Supplementation of α-KG restored all parameters of the OCR (Figure 7C; supplemental Figure 7A-D) and reduced the frequency of CD4$^+$FOXP3$^+$ cells in αCD3/αCD28-stimulated CD4$^+$CD25$^-$ cells obtained from APC^{high} mice (Figure 7D; supplemental Figure 7E).

The results obtained in APC^{high} mice demonstrate that chronically elevated aPC levels alter T-cell metabolism and induce FOXP3 expression. In our previous work[1] and the aforementioned analyses (Figures 1-6), we demonstrated that short-term stimulation of T cells with aPC in vitro is sufficient to alter T-cell metabolism and induce a Treg-like phenotype. To determine whether short-term stimulation with aPC is sufficient to alter T-cell metabolism and induce a Treg-like phenotype in vivo, we either injected aPC 3 times on alternate days (days 1, 3, and 5) and analyzed the mice on day 7, or we injected aPC only once and analyzed mice 48 hours later (Figure 7E). In both cases T-cell metabolism (OCR) was

Downloaded from http://ashpublications.net/bloodadvances/article-pdf/7/17/5055/2077006/blooda_adv-2023-010083-main.pdf by guest on 09 June 2024

Figure 5. α-KG or glutamine restores Treg-phenotype caused by aPC. (A) Bar graph with dot plot showing FOXP3 expression in human CD4+CD25− cells stimulated in an MLR (96 hours) (A, n = 4). Control CD4+CD25− cells (T) compared with CD4+CD25− cells preincubated with aPC (T + aPC) (1 hour, 20 nM) or with supplementation of α-KG (48 hours, 3.5 mM, T + aPC + α-KG) or glutamine (48 hours, 4 mM, T + aPC + Q). (B-C) Bar graphs with dot plots summarizing the expression of CD4+T-bet+ (B, n = 4) and CD4+IFNγ+ (C, n = 4) in CD4+CD25− cells in the MLR as estimated by flow cytometry and described in panel A. (D) Representative flow cytometry histograms (top) and bar graph with dot plot (bottom) reflecting the percentage of proliferating human CD4+CD25− cells in the MLR as described in panel A and quantified by CellTrace Violet cell proliferation dye (n = 5). (E) Representative flow cytometry plots and bar graph with dot plots of CD4+Ki-67+ cells after stimulation of human CD4+CD25− cells with plate-bound αCD3 and αCD28 for 96 hours and treated as described in panel A. The data are shown as the mean ± SEM, and statistical significance was determined by 1-way ANOVA for panels A-E: *$P < .05$, **$P < .01$, and ***$P < .005$.
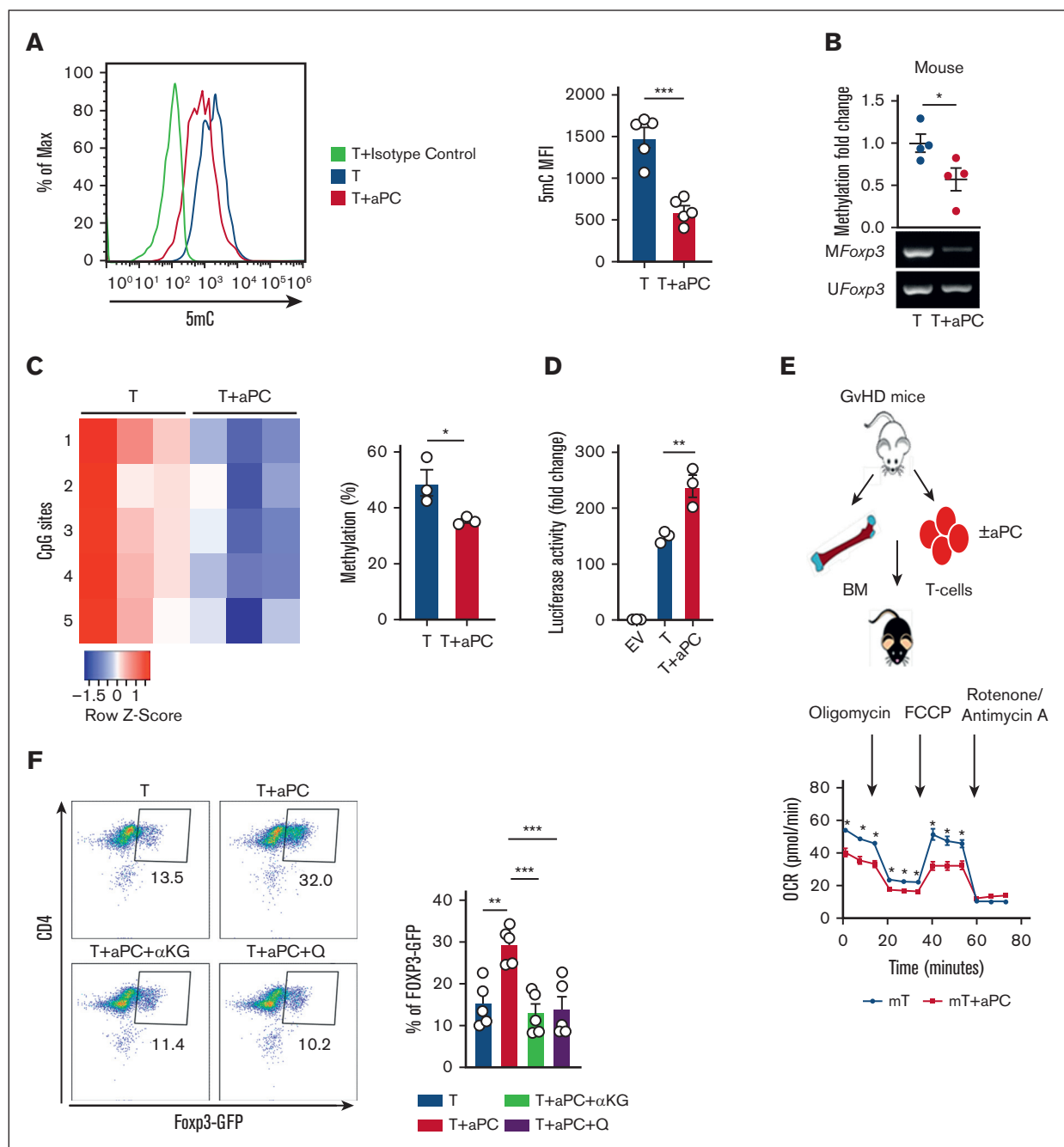
Figure 6. aPC induces epigenetic and metabolic alterations in mouse CD4+CD25− cells, resulting in a Treg-like phenotype. (A) 5mC (mouse, n = 4) analysis showing methylation alterations in CD4+CD25− cells without (T) or with aPC (T + aPC) preincubation followed by stimulation with αCD3 and αCD28 for 48 hours. A representative flow cytometry histogram (left) and a bar graph with a dot plot (right) summarizing data as the MFI. (B-C) Exemplary gel image of *Foxp3* promoter methylation (methylation-specific PCR, mouse; B, bottom, n = 4) and dot plot summarizing the results (B, top) of promoter methylation in CD4+CD25− cells without (T) or with aPC (T + aPC) preincubation (1 hour, 20 nM) followed by 48 hours of stimulation with αCD3 and αCD28. Heat map (C, left) and bar graph with dot plot (C, right) summarizing results of pyrosequencing of 5 CpG motifs in the *Foxp3* promoter in murine CD4+CD25− cells as described in panel B. Color code indicates the degree of methylation at each CpG motif, n = 3. (D) Bar graph with dot plot summarizing *Foxp3* promoter activity determined in EL4 murine T cells expressing *Foxp3* promoter−driven luciferase 24 hours after stimulation with αCD3 and αCD28 without (T) or with aPC (T + aPC) preincubation (n = 3). (E) T cells isolated from mice 2 weeks after induction of GVHD (E, top). T cells were preincubated with aPC (20 nM, 1 hour) before transplantation. Representative line graph showing (E, bottom) summarizing the results (E, n = 5). (F) Representative flow cytometry plot (top) and bar graph with dot plot (bottom) showing FOXP3 expression in T cells isolated from DEREG-GFP mice and stimulated with αCD3 and αCD28 (96 hours) (n = 5). Control CD4+ GFP− cells (T) compared with CD4+ GFP− cells preincubated with aPC (T + aPC, 1 hour, 20 nM) or with supplementation of α-KG (48 hours, 3.5 mM, T + aPC + α-KG) or glutamine (48 hours, 4 mM, T + aPC + Q). The data are shown as the mean ± SEM, and statistical significance was determined by 2-tailed Student t test for panels A-D and 1-way ANOVA for panel F: *P < .05, **P < .01, and ***P < .005; ns, nonsignificant.
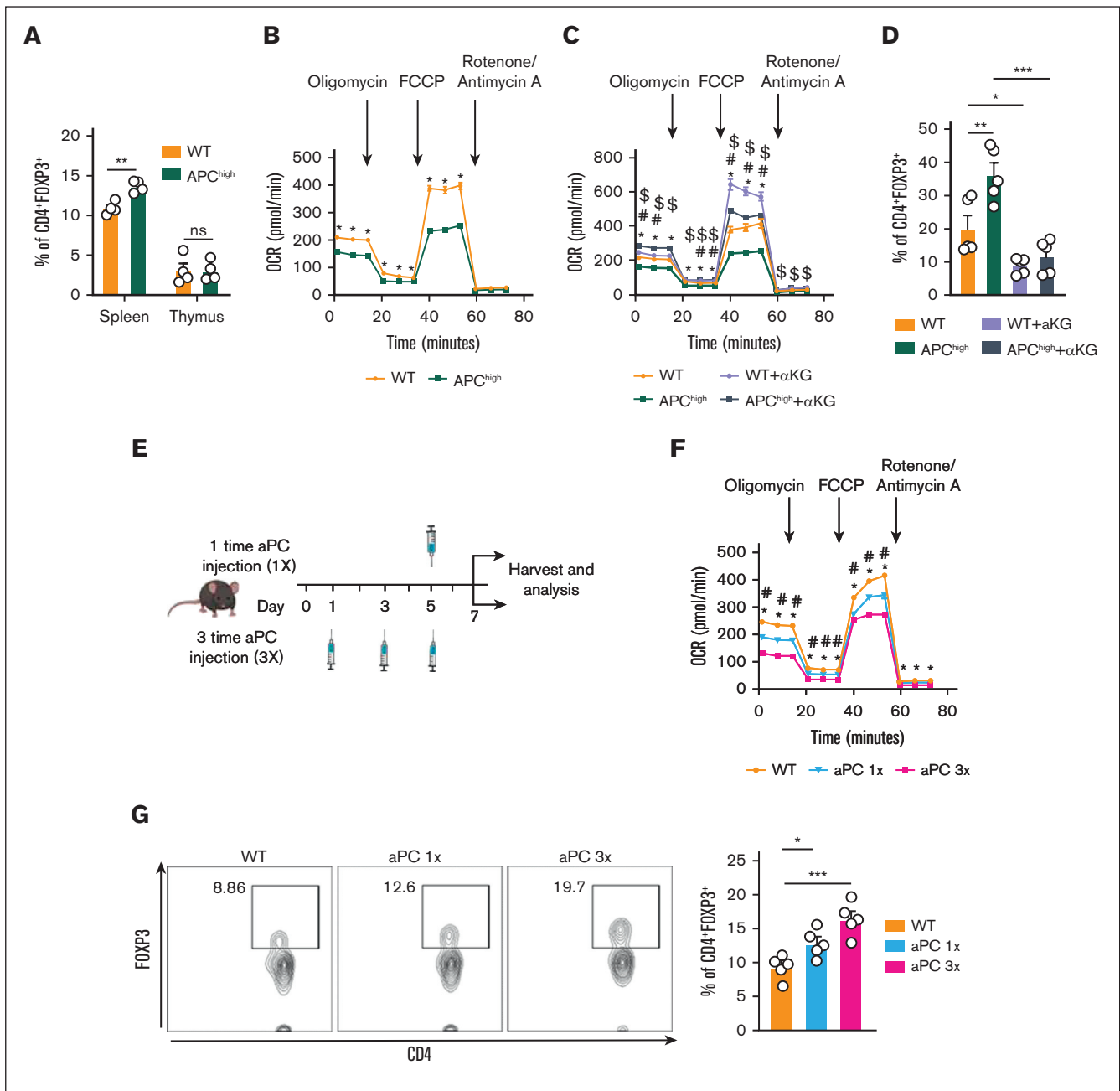
Figure 7. T-cell metabolism is homeostatically regulated by aPC, which induces Treg frequency in vivo. (A) Bar graph with dot plot showing the percentages of CD4+FOXP3+ cells in the spleen and thymus in WT and APC^{high} mice (flow cytometry) (n = 4). (B) Seahorse analysis showing the OCRs (line graph summarizing the results) in CD4+CD25− cells isolated from WT and APC^{high} mice and stimulated ex vivo with plate-bound αCD3 and αCD28 for 48 hours, n = 5. (C) Seahorse analysis showing the OCR (line graph summarizing the results) in CD4+CD25− isolated from WT and APC^{high} mice and stimulated ex vivo with plate-bound αCD3 and αCD28 without (APC^{high}) or with α-KG supplementation (48 hours, 3.5 mM, WT + α-KG; APC^{high} + α-KG). (D) Representative bar graph with dot plot summarizing CD4+FOXP3+ expression in CD4+CD25− cells isolated from WT and APC^{high} mice and stimulated with plate-bound αCD3 and αCD28 and experimental conditions as described in panel C (n = 5). (E) Schematic illustration of the experimental timeline and analysis. WT mice were injected once (1×) and 3 times (3×) with aPC (1 mg/kg). Control mice denoted later as WT were injected with PBS. (F) Seahorse analysis depicting the OCR (line graph summarizing results) in CD4+CD25− cells isolated from experimental mice as described in panel E, and stimulated ex vivo with plate-bound αCD3 and αCD28 for 48 hours. (G) Representative flow cytometry plots and bar graph with dot plot summarizing CD4+FOXP3+ expression in splenocytes− isolated from WT mice injected with PBS or aPC once (1×) or thrice (3×) (n = 5). The data are shown as the mean ± SEM; statistical significance was determined by 2-tailed Student t test for panel A; 2-way ANOVA for panels B-C,F; 1-way ANOVA for panels D,G. Significance is represented in panel B: *$P < .05$ (WT vs APC^{high}); panel C: *$P < .05$ (WT vs APC^{high}), #$P < .05$ (WT vs WT + α-KG), $\$P < .05$ (APC^{high} vs APC^{high} + α-KG); panel F: *$P < .05$ (WT vs aPC 1×), #$P < .05$ (WT vs aPC 3×); and panels A,D,G: *$P < .05$, **$P < .01$, and ***$P < .005$.

reduced and the frequency of CD4+FOXP3+ cells was increased in splenic T cells analyzed ex vivo (Figure 7F-G; supplemental Figure 8), corroborating results obtained in APC^high mice. Notably, aPC injection once was sufficient to reduce mitochondrial metabolism (OCR) and to increase the frequency of CD4+FOXP3+ cells (Figure 7F-G; supplemental Figure 8). The observed effects of aPC injections (once or thrice) on T-cell metabolism and FOXP3 expression corroborates a long-lasting effect of aPC on T cells, congruent with an epigenetic regulation of FOXP3.

Discussion

The cytoprotective functions of aPC, which are, at least in part, independent of its anticoagulant effects, are well established.[35,36] One of the unexplained findings regarding the cytoprotective effects of aPC is its long-lasting effect despite its short half-life in various in vivo models.[37-40] In the PROWESS study, the first study to evaluate the effect of aPC in patients with sepsis, the use of aPC during the first 3 days resulted in a survival benefit on day 28, indicating a prolonged protective effect of aPC also in humans.[41] Here, we provide a potential explanation for such long-lasting effects of aPC. Building on recent insights demonstrating that 1 hour preincubation of T cells is sufficient to dampen their activation, we demonstrate that aPC suppresses cellular metabolism, thus limiting the availability of metabolites required for epigenetic gene regulation, specifically of α-KG, which is necessary for FOXP3 and Treg induction. Upon supplementation with α-KG, aPC-induced Foxp3 promoter demethylation is reversed, reducing Foxp3 promoter activity and CD4+FOXP3+ cell abundance. Notably, aPC injection once into mice was sufficient to reduce mitochondrial metabolism (OCR) and to increase the abundance of CD4+FOXP3+ cells (Figure 7F-G; supplemental Figure 8). Considering the short half-life of aPC in vivo (~22 minutes) the observed effects on T-cell metabolism and FOXP3 expression, even after only a once-off aPC injection, corroborates a long-lasting effect of aPC on T cells, congruent with an epigenetic regulation of FOXP3. Taken together, we show that aPC promotes epigenetic reprogramming of T cells by dampening cellular metabolism and restricting metabolite availability. These results provide new insights into the effect of aPC on adaptive immunity and provide a possible explanation for the long-lasting effects of aPC observed in various disease models.

Evidence for epigenetic gene regulation by aPC has previously been obtained in models of chronic vascular disease. Thus, in the context of diabetes mellitus, aPC suppresses epigenetically sustained expression of p66^Shc in glomerular cells and plaque-associated macrophages and of p21 in tubular cells.[18,20] Suppression of epigenetically sustained p66^Shc and p21 expression by aPC is linked to DNMT1 induction.[19,20] Intriguingly, DNMT1 is linked to mitochondrial metabolism.[42,43] Hence, it is possible that the previously observed epigenetic gene regulation by aPC via DNMT1 is mechanistically linked to altered mitochondrial metabolism; however, this possibility needs to be addressed in future studies. Taken together, these results establish that aPC epigenetically controls gene expression, which appears to be linked to altered cellular metabolism.

Although this study provides a rationale for prolonged effects of aPC by demonstrating that aPC modulates cellular metabolism and thus epigenetically controls gene expression, the exact mechanisms through which aPC conveys these effects remain to be shown. A potential explanation is the reduced uptake of substrates from the extracellular milieu, as suggested by the reduced expression of amino acid transporters and GLUT1 and the reduced intracellular glucose and glutamine levels in the current study. Indeed, solute transporters including amino acid transporters and GLUT1 are considered "gatekeepers of immune cells," controlling their differentiation and function.[44] The function of Teffs depends on GLUT1 expression and increased glycolysis, and Teffs are characterized by an increased mitochondrial potential.[45-48] Congruently, GLUT1 deficiency, although having no impact on resting T cells in vivo, preferentially suppresses Teff development upon stimulation, for example, in the setting of experimental GVHD.[47] Conversely, inhibition of glycolysis, for example, by transforming growth factor β1, or reduced glucose uptake maintains FOXP3 expression, increases Treg abundance, and maintains their immunosuppressive function.[13,14,49] In this study we show normal T-cell development but induction of CD4+FOXP3+ cells in APC^high mice, in stimulated CD4+CD25− cells, and in stimulated naïve T cells preincubated with aPC. The induction of CD4+FOXP3+ cells is associated with reduced GLUT1 expression and reduced pyruvate and α-KG levels.

Deficiency of α-KG can be compensated by an anaplerotic reaction providing glutamate as a substrate for α-KG. aPC reduces the expression of 2 major amino acid transporters, ASCT2 and SNAT1, and lowers intracellular glutamine levels in T cells, suggesting that this pathway to restore α-KG levels is likewise suppressed by aPC. Glutamine, which fuels this anaplerotic reaction, suppresses FOXP3 expression and Treg induction.[16] Conversely, limited glutamine supply and reduced α-KG levels are sufficient to promote Treg development, immunosuppressive cytokines, and resolution of inflammation.[16] These and the current observations, together with the previous finding that aPC dampens aGVHD by induction of Tregs[1] support a model in which aPC promotes Treg development by reducing substrate uptake (glucose and glutamine), glycolysis, and TCA-activity in T cells (Figure 7). As α-KG–dependent suppression of Tregs has been recently linked to increased de novo lipid biosynthesis,[22] further studies should address whether aPC modulates other metabolic pathways in T cells such as lipid biosynthesis.

An eminent question is whether the observed effects of aPC on cellular metabolism and epigenetic gene regulation are specific for aPC. Thrombin has been reported to alter metabolites in macrophages and platelets, suggesting that other coagulation proteases may convey similar effects.[50,51] Furthermore, loss of endothelial thrombomodulin expression and reduced aPC levels have not only been observed in GVHD but also in other diseases associated with endothelial dysfunction, such as atherosclerosis, diabetes mellitus, and sepsis.[3,19,52] Whether reduced aPC levels and dysbalanced coagulation activity with increased prothrombotic activity translates into altered cellular metabolism and epigenetic gene regulation in these diseases remain to be shown.

Here, we have demonstrated that aPC modulates T-cell metabolism and thus T-cell differentiation. These data support a concept in which altered coagulation protease activity contributes to a specific micromilieu affecting cellular metabolism and differentiation of T cells. Further work is required to characterize the effect of altered coagulation protease activity, not only on immune cells but also in other cells.

Acknowledgments

Authorship

Contribution: D.G. designed, performed, and interpreted the results of the in vivo, in vitro, and ex vivo experiments, and prepared the manuscript; A.E., S.R., M.K.P., S. Kohli, S.A., K.S., S. Krishnan, and R.R. supported the mouse experiments and in vitro and ex vivo analysis; U.C. conducted and interpreted amino acid analysis; M.K. assisted in pyrosequencing experiments and data interpretation; R.H. provided human blood samples; and B.I. designed and interpreted the experimental work, and prepared the manuscript.

Conflict-of-interest disclosure: The authors declare no competing financial interests.

ORCID profiles: A.E., 0000-0001-6784-8370; M.K., 0000-0003-4026-8530; S.K., 0000-0003-2118-7380; B.I., 0000-0003-0714-6160.

Correspondence: Berend Isermann, Universitätsklinikum Leipzig AöR, Institut für Laboratoriumsmedizin, Klinische Chemie und Molekulare Diagnostik, Paul-List-Straße 13-15; 04103 Leipzig, Germany; email: berend.isermann@medizin.uni-leipzig.de.

References

1. Ranjan S, Goihl A, Kohli S, et al. Activated protein C protects from GvHD via PAR2/PAR3 signalling in regulatory T-cells. *Nat Commun*. 2017;8(1):311.

2. Sinha RK, Flynn R, Zaiken M, et al. Activated protein C ameliorates chronic graft-versus-host disease by PAR1-dependent biased cell signaling on T cells. *Blood*. 2019;134(9):776-781.

3. Andrulis M, Dietrich S, Longerich T, et al. Loss of endothelial thrombomodulin predicts response to steroid therapy and survival in acute intestinal graft-versus-host disease. *Haematologica*. 2012;97(11):1674-1677.

4. Ito T, Maruyama I. Thrombomodulin: protectorate God of the vasculature in thrombosis and inflammation. *J Thromb Haemost*. 2011;9(suppl 1):168-173.

5. Dumitru C, Kabat AM, Maloy KJ. Metabolic adaptations of CD4(+) T cells in inflammatory disease. *Front Immunol*. 2018;9:540.

6. Blagih J, Hennequart M, Zani F. Tissue nutrient environments and their effect on regulatory T cell biology. *Front Immunol*. 2021;12:637960.

7. Loftus RM, Finlay DK. Immunometabolism: cellular metabolism turns immune regulator. *J Biol Chem*. 2016;291(1):1-10.

8. Chao T, Wang H, Ho PC. Mitochondrial control and guidance of cellular activities of T cells. *Front Immunol*. 2017;8:473.

9. Michalek RD, Gerriets VA, Jacobs SR, et al. Cutting edge: distinct glycolytic and lipid oxidative metabolic programs are essential for effector and regulatory CD4+ T cell subsets. *J Immunol*. 2011;186(6):3299-3303.

10. Chang CH, Curtis JD, Maggi LB Jr, et al. Posttranscriptional control of T cell effector function by aerobic glycolysis. *Cell*. 2013;153(6):1239-1251.

11. Gerriets VA, Kishton RJ, Nichols AG, et al. Metabolic programming and PDHK1 control CD4+ T cell subsets and inflammation. *J Clin Invest*. 2015; 125(1):194-207.

12. Buck MD, Sowell RT, Kaech SM, Pearce EL. Metabolic instruction of immunity. *Cell*. 2017;169(4):570-586.

13. Shi LZ, Wang R, Huang G, et al. HIF1alpha-dependent glycolytic pathway orchestrates a metabolic checkpoint for the differentiation of TH17 and Treg cells. *J Exp Med*. 2011;208(7):1367-1376.

14. Watson MJ, Vignali PDA, Mullett SJ, et al. Metabolic support of tumour-infiltrating regulatory T cells by lactic acid. *Nature*. 2021;591(7851):645-651.

15. Chisolm DA, Savic D, Moore AJ, et al. CCCTC-binding factor translates interleukin 2- and alpha-ketoglutarate-sensitive metabolic changes in T cells into context-dependent gene programs. *Immunity*. 2017;47(2):251-267.e7.

16. Klysz D, Tai X, Robert PA, et al. Glutamine-dependent alpha-ketoglutarate production regulates the balance between T helper 1 cell and regulatory T cell generation. *Sci Signal*. 2015;8(396):ra97.

17. Zdzisińska B, Żurek A, Kandefer-Szerszeń M. Alpha-ketoglutarate as a molecule with pleiotropic activity: well-known and novel possibilities of therapeutic use. *Arch Immunol Ther Exp*. 2017;65(1):21-36.

18. Bock F, Shahzad K, Wang H, et al. Activated protein C ameliorates diabetic nephropathy by epigenetically inhibiting the redox enzyme p66Shc. *Proc Natl Acad Sci U S A*. 2013;110(2):648-653.

19. Shahzad K, Gadi I, Nazir S, et al. Activated protein C reverses epigenetically sustained p66(Shc) expression in plaque-associated macrophages in diabetes. *Commun Biol*. 2018;1:104.

20. Al-Dabet MM, Shahzad K, Elwakiel A, et al. Reversal of the renal hyperglycemic memory in diabetic kidney disease by targeting sustained tubular p21 expression. *Nat Commun*. 2022;13(1):5062.

21. Xu T, Stewart KM, Wang X, et al. Metabolic control of TH17 and induced Treg cell balance by an epigenetic mechanism. *Nature*. 2017;548(7666): 228-233.

22. Matias MI, Yong CS, Foroushani A, et al. Regulatory T cell differentiation is controlled by alphaKG-induced alterations in mitochondrial metabolism and lipid homeostasis. *Cell Rep*. 2021;37(5):109911.

23. Isermann B, Vinnikov IA, Madhusudhan T, et al. Activated protein C protects against diabetic nephropathy by inhibiting endothelial and podocyte apoptosis. *Nat Med*. 2007;13(11):1349-1358.

24. Lahl K, Sparwasser T. In vivo depletion of FoxP3+ Tregs using the DEREG mouse model. *Methods Mol Biol*. 2011;707:157-172.

25. Wang J, Ioan-Facsinay A, van der Voort EI, Huizinga TW, Toes RE. Transient expression of FOXP3 in human activated nonregulatory CD4+ T cells. *Eur J Immunol*. 2007;37(1):129-138.

26. Mikami N, Kawakami R, Chen KY, Sugimoto A, Ohkura N, Sakaguchi S. Epigenetic conversion of conventional T cells into regulatory T cells by CD28 signal deprivation. *Proc Natl Acad Sci U S A*. 2020;117(22):12258-12268.

27. Chapman NM, Boothby MR, Chi H. Metabolic coordination of T cell quiescence and activation. *Nat Rev Immunol*. 2020;20(1):55-70.

28. Johnson MO, Wolf MM, Madden MZ, et al. Distinct regulation of Th17 and Th1 cell differentiation by glutaminase-dependent metabolism. *Cell*. 2018; 175(7):1780-1795.e19.

29. Kono M, Yoshida N, Maeda K, Tsokos GC. Transcriptional factor ICER promotes glutaminolysis and the generation of Th17 cells. *Proc Natl Acad Sci U S A*. 2018;115(10):2478-2483.

30. Araujo L, Khim P, Mkhikian H, Mortales CL, Demetriou M. Glycolysis and glutaminolysis cooperatively control T cell function by limiting metabolite supply to N-glycosylation. *Elife*. 2017;6:e21330.

31. Yoo HC, Yu YC, Sung Y, Han JM. Glutamine reliance in cell metabolism. *Exp Mol Med*. 2020;52(9):1496-1516.

32. Carr EL, Kelman A, Wu GS, et al. Glutamine uptake and metabolism are coordinately regulated by ERK/MAPK during T lymphocyte activation. *J Immunol*. 2010;185(2):1037-1044.

33. Nakaya M, Xiao Y, Zhou X, et al. Inflammatory T cell responses rely on amino acid transporter ASCT2 facilitation of glutamine uptake and mTORC1 kinase activation. *Immunity*. 2014;40(5):692-705.

34. Ren W, Liu G, Yin J, et al. Amino-acid transporters in T-cell activation and differentiation. *Cell Death Dis*. 2017;8(3):e2655.

35. Griffin JH, Zlokovic BV, Mosnier LO. Activated protein C: biased for translation. *Blood*. 2015;125(19):2898-2907.

36. Bock F, Shahzad K, Vergnolle N, Isermann B. Activated protein C based therapeutic strategies in chronic diseases. *Thromb Haemost*. 2014;111(4): 610-617.

37. Cheng T, Liu D, Griffin JH, et al. Activated protein C blocks p53-mediated apoptosis in ischemic human brain endothelium and is neuroprotective. *Nat Med*. 2003;9(3):338-342.

38. Kerschen E, Hernandez I, Zogg M, et al. Activated protein C targets CD8+ dendritic cells to reduce the mortality of endotoxemia in mice. *J Clin Invest*. 2010;120(9):3167-3178.

39. Nazir S, Gadi I, Al-Dabet MM, et al. Cytoprotective activated protein C averts Nlrp3 inflammasome-induced ischemia-reperfusion injury via mTORC1 inhibition. *Blood*. 2017;130(24):2664-2677.

40. Kant R, Halder SK, Fernandez JA, Griffin JH, Milner R. Activated protein C attenuates experimental autoimmune encephalomyelitis progression by enhancing vascular integrity and suppressing microglial activation. *Front Neurosci*. 2020;14:333.

41. Bernard GR, Vincent JL, Laterre PF, et al. Efficacy and safety of recombinant human activated protein C for severe sepsis. *N Engl J Med*. 2001;344(10): 699-709.

42. Maresca A, Del Dotto V, Capristo M, et al. DNMT1 mutations leading to neurodegeneration paradoxically reflect on mitochondrial metabolism. *Hum Mol Genet*. 2020;29(11):1864-1881.

43. Park YJ, Lee S, Lim S, et al. DNMT1 maintains metabolic fitness of adipocytes through acting as an epigenetic safeguard of mitochondrial dynamics. *Proc Natl Acad Sci U S A*. 2021;118(11):e2021073118.

44. Song W, Li D, Tao L, Luo Q, Chen L. Solute carrier transporters: the metabolic gatekeepers of immune cells. *Acta Pharm Sin B*. 2020;10(1):61-78.

45. Sukumar M, Liu J, Mehta GU, et al. Mitochondrial membrane potential identifies cells with enhanced stemness for cellular therapy. *Cell Metab*. 2016; 23(1):63-76.

46. Court AC, Le-Gatt A, Luz-Crawford P, et al. Mitochondrial transfer from MSCs to T cells induces Treg differentiation and restricts inflammatory response. *EMBO Rep*. 2020;21(2):e48052.

47. Macintyre AN, Gerriets VA, Nichols AG, et al. The glucose transporter Glut1 is selectively essential for CD4 T cell activation and effector function. *Cell Metab*. 2014;20(1):61-72.

48. Hochrein SM, Wu H, Eckstein M, et al. The glucose transporter GLUT3 controls T helper 17 cell responses through glycolytic-epigenetic reprogramming. *Cell Metab*. 2022;34(4):516-532.e11.

49. Chen X, Feng L, Li S, Long D, Shan J, Li Y. TGF-beta1 maintains Foxp3 expression and inhibits glycolysis in natural regulatory T cells via PP2A-mediated suppression of mTOR signaling. *Immunol Lett*. 2020;226:31-37.

50. Ukan U, Delgado Lagos F, Kempf S, et al. Effect of thrombin on the metabolism and function of murine macrophages. *Cells*. 2022;11(10):1718.

51. Ravi S, Chacko B, Sawada H, et al. Metabolic plasticity in resting and thrombin activated platelets. *PLoS One*. 2015;10(4):e0123597.

52. Faust SN, Levin M, Harrison OB, et al. Dysfunction of endothelial protein C activation in severe meningococcal sepsis. *N Engl J Med*. 2001;345(6): 408-416.